2018 European Control Conference (ECC)
June 12-15, 2018. Limassol, Cyprus

A General Admittance Control Approach for Indirect Force Control of Industrial Manipulators

Silke Klose, Arne Wahrburg, Debora Clever, Hao Ding

***Abstract*— A novel indirect force control scheme for rigid manipulators is presented. The approach is based on well-known proportional Cartesian force controllers. However, the new concept integrates Cartesian force control and mapping from Cartesian- to joint-space into a dynamic state-space controller. This allows interpreting the tasks of force controller parameterization and mapping to joint space as an eigenstructure assignment problem. Guidelines for practical force controller tuning are given. The proposed control approach has been verified in several experimental results gathered on an ABB YuMi, a redundant dual-arm manipulator.**

I. INTRODUCTION

Traditionally, position control has been the key focus for industrial manipulators, with high speed, repeatability, and path accuracy being main objectives. Purely position controlled approaches work well in highly structured environments. However, industrial robots are more and more facing at least partially unstructured environments and a demand for interactive usage [1]. In such circumstances, unexpected contact situations may occur and pure position control is prone to fail. As a remedy, combined force and motion control schemes can be employed. Examples of applications requiring force control are assembly, polishing, grinding, and also physical human-robot interaction.

Two popular approaches for indirect force and interaction control are represented by impedance and admittance control schemes [2], [3]. In impedance control motor torques are generated as a reaction to position and/or velocity deviations (*position in - force out*). Such approaches have been shown to be suitable for stable contact situations [4]. However, the achievable accuracy in position controlled directions is limited. In admittance control schemes, position or velocity references are generated as a reaction to forces (*force in - position out*). As the output of an admittance controller is a position or velocity reference, existing position control loops can be employed, making it attractive for industrial applications. While it is known that maintaining stability in stiff contact situations is challenging [5, Section 1.3.2], accuracy in position controlled directions can be very high due to the maturity of cascaded motion control structures in robot controllers.

A standard admittance controller is described by

$$\dot{x}_{\text{ref}} = -D^{-1} f, \tag{1}$$

where $\dot{x}_{\text{ref}}$ is the reference velocity generated by the indirect force controller, f is the actual force, and D is a gain factor referred to as *damping* [6, Section 7.2]. This approach – also known as *Cartesian Damping* – requires a design trade-off. A small force controller gain, i.e. large damping D, is known to result in stable behavior even in stiff contact situations. However, it leads to small force control bandwidth and results in large interaction forces that might damage the environment and/or the manipulator. While high force control gains, i.e. low damping D, cures the latter, it can easily make the robot unstable in contact situations. Several approaches have been reported to mitigate the aforementioned problem. They include oscillation observers and cancellation schemes [7], additional derivative controller action [8], [9], controller gain adaptation [10], [11], [12], sliding mode control [13], and model-predictive control approaches [14], [15].

Against this background, the contribution of this paper is twofold. Firstly, a state-space description of the overall system is given, consisting of Cartesian force controller, mapping from Cartesian space to joint space, the position controlled manipulator, and the environment. This allows to systematically analyze stability of different force control approaches based on a linearization of the overall system. Secondly, a novel admittance-type force controller is introduced. This *Generalized Admittance Controller* (GAC) combines the Cartesian force controller and the mapping to joint space into a dynamic state-space controller. Thereby, well-established design approaches such as eigenstructure assignment can be employed for controller design. The effectiveness of the new control approach is demonstrated by experimental results obtained on an ABB YuMi, a dual-arm manipulator with 7 degrees of freedom in each arm.

The paper is structured as follows. In Section II, a problem description is given and basic assumptions with respect to the manipulator dynamics are discussed. While Section III briefly recapitulates standard proportional-type Cartesian force control, the proposed new controller scheme is presented in Section IV. In Section V, experimental results are discussed, before a conclusion is given in Section VI.

II. PRELIMINARIES

We consider the dynamics of a rigid-link N_{dof} degrees of freedom robotic manipulator described by

$$\mathbf{M}(\mathbf{q})\ddot{\mathbf{q}} + \mathbf{C}(\mathbf{q},\dot{\mathbf{q}})\dot{\mathbf{q}} + \mathbf{G}(\mathbf{q}) + \boldsymbol{\tau}_{\text{fric}} + \boldsymbol{\tau}_{\text{ext}} = \boldsymbol{\tau}_{\text{mot}} \tag{2}$$

with the joint angles $\mathbf{q} \in \mathbb{R}^{N_{\text{dof}}}$, the inertia matrix $\mathbf{M}(\mathbf{q})$, the centrifugal and Coriolis matrix $\mathbf{C}(\mathbf{q},\dot{\mathbf{q}})$, the gravity $\mathbf{G}(\mathbf{q})$ as

The authors are with the ABB Corporate Research Center, GERMANY, silke.klose; arne.wahrburg; debora.clever; hao.ding/@de.abb.com

well as the friction $\boldsymbol{\tau}_{\text{fric}}$ and motor torques $\boldsymbol{\tau}_{\text{mot}}$. The term $\boldsymbol{\tau}_{\text{ext}}$ describes the joint torques induced by external loads.

In this paper, it is assumed that only the tool center point (TCP) has contact with the environment. This is typical for many robotic applications like assembly, grinding or polishing. Consequently the torques induced in the joints are

$$\boldsymbol{\tau}_{\text{ext}} = \mathbf{J}^T(\mathbf{q})\mathbf{f}, \text{ with } \mathbf{f} = \begin{bmatrix} f_x, & f_y, & f_z, & \tau_x, & \tau_y, & \tau_z \end{bmatrix}^T, \quad (3)$$

where $\mathbf{f}$ is the *wrench* summarizing the contact forces and torques in the Cartesian domain and $\mathbf{J}(\mathbf{q})$ is the manipulator TCP Jacobian with respect to the base frame.

Traditionally, industrial manipulators are position controlled at joint level. Then, force control can be realized as an additional outer loop generating a position offset $\Delta\mathbf{q}_{\text{ref}}$ corresponding to the force control error (see Figure 1). One approach for the position control is a jointwise P-PI-cascade combined with gravity and friction compensation. It can be verified by experiments (reference step responses), that with well-tuned P-PI-parameters the inner loop can be sufficiently approximated by a linear decoupled N_{dof}-th order system

$$\dot{\mathbf{q}}_{\text{act}} = \underbrace{\text{diag}\left[-\frac{1}{T_1},\ldots,-\frac{1}{T_{N_{\text{dof}}}}\right]}_{\mathbf{A}}\mathbf{q}_{\text{act}} + \underbrace{\text{diag}\left[\frac{1}{T_1},\ldots,\frac{1}{T_{N_{\text{dof}}}}\right]}_{\mathbf{B}}\tilde{\mathbf{q}}_{\text{ref}}, \quad (4)$$

where $\mathbf{q}_{\text{act}}$ is the actual and $\tilde{\mathbf{q}}_{\text{ref}}$ the reference joint configuration. The time constants $T_1,\ldots,T_{N_{\text{dof}}}$ are independent of the actual joint configuration. The Cartesian contact force is modelled as

$$\mathbf{f} = \mathbf{K}_e(\mathbf{q}_{\text{act}})(\mathbf{x}_{\text{act}} - \mathbf{x}_{\text{cont}}) = \mathbf{K}_e(\mathbf{q}_{\text{act}})(\boldsymbol{\Psi}(\mathbf{q}_{\text{act}}) - \boldsymbol{\Psi}(\mathbf{q}_{\text{cont}})), \quad (5)$$

where $\mathbf{q}_{\text{cont}}$ is the robot's joint angle configuration at first contact with the stiff environment. $\mathbf{x}_{\text{cont}}$ results from the robot forward kinematics $\boldsymbol{\Psi}(\mathbf{q}_{\text{cont}})$. The matrix $\mathbf{K}_e(\mathbf{q}_{\text{act}})$ represents the 6-dimensional Cartesian stiffness matrix which is a series connection of the (constant) environmental stiffness and the robot's stiffness depending on the actual joint configuration. In case of high environmental stiffness (e.g. metal surfaces) $\mathbf{K}_e(\mathbf{q}_{\text{act}})$ is dominated by the robot's stiffness. The robot's stiffness must be either identified or can be gained by a robot model.

Linearizing the contact force model (5) at $\Delta\mathbf{q}_{\text{act}} = \mathbf{q}_{\text{act}} - \mathbf{q}_{\text{cont}}$ yields

$$\Delta\mathbf{f} = \mathbf{f} - \underbrace{\mathbf{f}_{\text{cont}}}_{=\mathbf{0}} = \underbrace{\mathbf{K}_e(\mathbf{q}_{\text{cont}})}_{\equiv\mathbf{K}_e}\mathbf{J}(\mathbf{q}_{\text{cont}})\Delta\mathbf{q}_{\text{act}}. \quad (6)$$

Hence, the linearized contact force is a function of the Jacobian at $\mathbf{q}_{\text{cont}}$. Either the wrench $\mathbf{f}$ can be measured directly by a 6-DOF force/ torque sensor or it must be estimated by a force observer [16], [17].

III. Cartesian Damping as classical Admittance Control Structure (CD)

One of the most common approaches to force control is to generate a Cartesian speed offset from

$$\Delta\dot{\mathbf{x}}_{ref} = \mathbf{D}^{-1}\mathbf{S}(\mathbf{f}_{\text{ref}} - \mathbf{f}), \quad (7)$$

with the damping matrix $\mathbf{D}$ and the diagonal selection matrix $\mathbf{S}$ enabling force control in desired Cartesian direction by setting the corresponding diagonal element in $\mathbf{S}$ to 1. Due to $\mathbf{D}\Delta\dot{\mathbf{x}}_{\text{ref}} = \mathbf{S}(\mathbf{f}_{\text{ref}} - \mathbf{f})$, the gain $\mathbf{D}$ can be interpreted as a damping factor. Therefore, the approach is termed "Cartesian Damping" (CD) in this paper.

The force control with CD comprises three independent steps, each of which can be designed, analyzed and implemented separately (see Figure 1):

1) Force control law in Cartesian domain (7)
2) Mapping Cartesian speed offset $\Delta\dot{\mathbf{x}}_{ref}$ to joint-space using the (pseudo)inverse of the manipulator's Jacobian, i.e. $\Delta\dot{\mathbf{q}}_{\text{ref}} = \mathbf{J}^+(\mathbf{q}_{\text{act}})\Delta\dot{\mathbf{x}}_{\text{ref}}$. Here it must be guaranteed that the manipulator does not run into any singularity[1]
3) Time integration of speed offset in joint-space to get position offset $\Delta\mathbf{q}_{\text{ref}}$

As discussed in Section I the tuning of the damping matrix $\mathbf{D}$ is a trade-off between reference response speed and oscillations up to bouncing effects. Because the control structure has a N_{dof}-dimensional integrator (see Figure 1), the CD-controller has steady-state convergence to reference forces.

IV. General Admittance Control (GAC)

The General Admittance Control (GAC) combines the three steps of the CD controller discussed in Section III into a dynamic controller

$$\dot{\boldsymbol{\xi}} = \mathbf{A}_1\boldsymbol{\xi} + \mathbf{J}^+(\mathbf{q}_{\text{act}})\mathbf{B}_1\mathbf{e} \quad (8)$$

$$\Delta\mathbf{q}_{ref} = \mathbf{C}_1\boldsymbol{\xi} + \mathbf{D}_1\mathbf{J}^T(\mathbf{q}_{\text{act}})\mathbf{f}, \quad (9)$$

where $\boldsymbol{\xi}$ is the internal controller state, the force error $\mathbf{e} = \mathbf{f}_{\text{ref}} - \mathbf{f}$ the input, the force $\mathbf{f}$ the feedthrough term and the reference joint angles offset $\Delta\mathbf{q}_{\text{ref}}$ the ouput of GAC. Hence, mapping to joint-space and (in case of 7-DOF manipulators) redundancy resolution are embedded into the force/admittance controller. The explicit introduction of the (pseudo)inverse of the Jacobian in the state differential equation (8) is motivated by the idea to take the CD structure as basis for the controller design. The explicit introduction of the Jacobian transpose in the output function (9) is needed for Cartesian wrench mapping to joint torques. The closed-loop structure is shown in Figure 1.

The following subsections are organized as follows. In Subsection IV-A the GAC closed-loop dynamics is reformulated as a linear fictive system with a fictive state-space controller. Here conditional equations for the GAC controller matrices $\mathbf{A}_1$, $\mathbf{B}_1$, $\mathbf{C}_1$ and $\mathbf{D}_1$ depending on the fictive state-space controller are derived. In Subsection IV-B the equivalence of CD and GAC is discussed. For the synthesis of the fictive state-space controller the *Complete Modal Control* is taken. All relevant formulars of the *Complete Modal Control* are summarized in Subsection IV-C. Based on the

[1] A pseudoinverse with $\mathbf{J}(\mathbf{q})\mathbf{J}^+(\mathbf{q}) = \mathbf{I}_6$ where $\mathbf{I}_6$ is the six-dimensional identity matrix is needed in case of 7-DOF manipulators (7-DOF $\equiv$ 7 joints) e.g. ABB YuMi (see V). For classcial 6-DOF robots $\mathbf{J}^{(-1)}(\mathbf{q}_{\text{act}})$ can be employed.

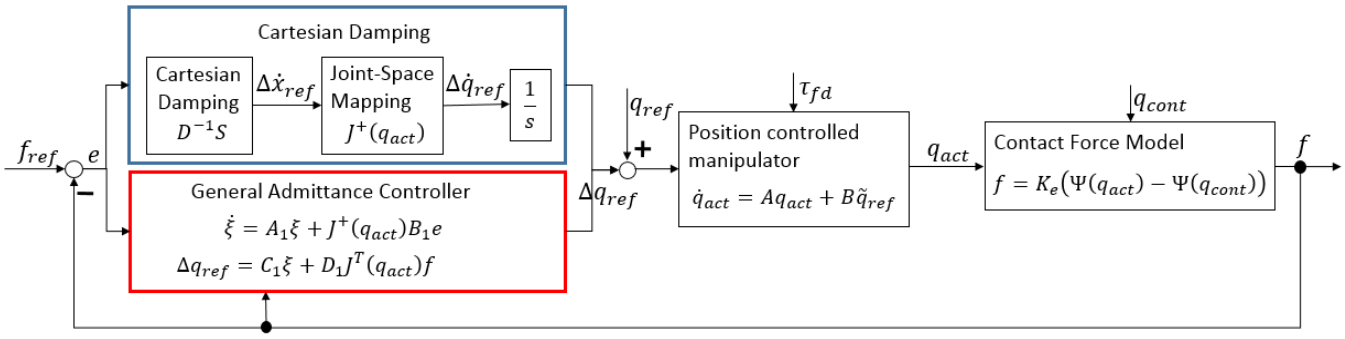

Fig. 1: Closed-loop structure with admittance control, position controlled manipulator (robot's dynamics, P-PI-cascade and gravity compensation) and contact force model; Comparison of different admittance control structures: Cartesian Damping (CD) in the blue box and General Admittance Control (GAC) in the red box

results of IV-B and the selected controller synthesis in IV-C a tuning formular for the GAC parameters is proposed in Subsection IV-D.

A. GAC closed-loop dynamics

If the approximated robot dynamics (4) is considered at

$$\Delta\mathbf{q}_{\text{act}} = \mathbf{q}_{\text{act}} - \mathbf{q}_{\text{cont}} \tag{10}$$

$$\begin{aligned}\Delta\tilde{\mathbf{q}}_{\text{ref}} &= \tilde{\mathbf{q}}_{\text{ref}} - \tilde{\mathbf{q}}_{\text{ref,cont}} \\ &= \mathbf{q}_{\text{ref}} + \Delta\mathbf{q}_{\text{ref}} - (\mathbf{q}_{\text{ref,cont}} - \underbrace{\Delta\mathbf{q}_{\text{ref,cont}}}_{=\mathbf{0}})\end{aligned} \tag{11}$$

and the linearized contact force (6) is taken into account, then the entire closed-loop dynamics can be written as

$$\begin{bmatrix}\Delta\dot{\mathbf{q}}_{\text{act}} \\ \dot{\boldsymbol{\xi}}\end{bmatrix} = \underbrace{\begin{bmatrix}\mathbf{A} + \mathbf{B}\mathbf{D}_1\mathbf{J}^T(\mathbf{q}_{\text{act}})\mathbf{K}_e\mathbf{J}(\mathbf{q}_{\text{cont}}) & \mathbf{B}\mathbf{C}_1 \\ -\mathbf{J}^{+}(\mathbf{q}_{\text{act}})\mathbf{B}_1\mathbf{K}_e\mathbf{J}(\mathbf{q}_{\text{cont}}) & \mathbf{A}_1\end{bmatrix}}_{\mathbf{A}_g}\begin{bmatrix}\Delta\mathbf{q}_{\text{act}} \\ \boldsymbol{\xi}\end{bmatrix} + \begin{bmatrix}\mathbf{0} \\ \mathbf{J}^{+}(\mathbf{q}_{\text{act}})\mathbf{B}_1\end{bmatrix}\mathbf{f}_{\text{ref}} + \begin{bmatrix}\mathbf{B} \\ \mathbf{0}\end{bmatrix}(\mathbf{q}_{\text{ref}} - \mathbf{q}_{\text{ref,cont}}), \tag{12}$$

$$\Delta\mathbf{q}_{\text{ref}} = \begin{bmatrix}\mathbf{D}_1\mathbf{J}^T(\mathbf{q}_{\text{act}})\mathbf{K}_e\mathbf{J}(\mathbf{q}_{\text{cont}}) & \mathbf{C}_1\end{bmatrix}\begin{bmatrix}\Delta\mathbf{q}_{\text{act}} \\ \boldsymbol{\xi}\end{bmatrix}. \tag{13}$$

The system matrix $\mathbf{A}_g$ depending on the GAC controller matrices $\mathbf{A}_1$, $\mathbf{B}_1$, $\mathbf{C}_1$ and $\mathbf{D}_1$ can be rewritten as classical linear state-space controller problem for the fictive system

$$\mathbf{A}_g = \underbrace{\begin{bmatrix}\mathbf{A} & \mathbf{0} \\ -\mathbf{J}^{+}(\mathbf{q}_{\text{act}})\mathbf{B}_1\mathbf{K}_e\mathbf{J}(\mathbf{q}_{\text{cont}}) & \mathbf{A}_1\end{bmatrix}}_{\mathbf{A}_f} - \underbrace{\begin{bmatrix}\mathbf{B} \\ \mathbf{0}\end{bmatrix}}_{\mathbf{B}_f}\underbrace{\begin{bmatrix}-\mathbf{D}_1 & -\mathbf{C}_1\end{bmatrix}\begin{bmatrix}\mathbf{J}^T(\mathbf{q}_{\text{act}})\mathbf{K}_e\mathbf{J}(\mathbf{q}_{\text{cont}}) & \mathbf{0} \\ \mathbf{0} & \mathbf{I}\end{bmatrix}}_{\mathbf{R}_f = \begin{bmatrix}\mathbf{R}_{f1} & \mathbf{R}_{f2}\end{bmatrix}}. \tag{14}$$

With (14), the GAC controller design can be conducted in three steps:

1) Definition of $\mathbf{A}_1$ and $\mathbf{B}_1$
2) Calculation of $\mathbf{R}_f$
3) Calculation of $\mathbf{C}_1$ and $\mathbf{D}_1$ from $\mathbf{R}_f$

It is pointed out, that the fictive system matrix $\mathbf{A}_f$ and state-space controller $\mathbf{R}_f$ depend on $\mathbf{q}_{\text{act}}$ and are therefore time-variant. Consequently controller design methods for time-variant systems must be used for calculation of $\mathbf{R}_f$ to guarantee mathematically predefined requirements of the closed-loop dynamics like stability, performance and robustness. For the sake of simplicity and ease-of-use, the controller design is done for the case $\mathbf{q}_{\text{act}} = \mathbf{q}_{\text{cont}}$. Hence, linear time-invariant methods with all their benefits can be used. This simplification is justified, as the robot's configuration only changes smoothly (and slowly compared to the controller dynamics) in practical contact applications. The controller design method for $\mathbf{R}_f$ used in this paper is explained in Section IV-C.

Independent of the controller synthesis for $\mathbf{R}_f$, the GAC controller matrices $\mathbf{A}_1$ and $\mathbf{B}_1$ must be defined first to get a defined fictive system matrix $\mathbf{A}_f$. To achieve steady-state convergence of the closed-loop for piecewise constant feedforward and disturbance signals, the matrices $\mathbf{A}_1$ and $\mathbf{B}_1$ are defined as

$$\mathbf{A}_1 = \mathbf{0},\ \mathbf{B}_1 = \mathbf{I}. \tag{15}$$

If steady-state convergence is desired for other frequencies (e.g. harmonics), $\mathbf{A}_1$ and $\mathbf{B}_1$ must be adapted accordingly. Hence, the ansatz GAC (8) can respect different kind of signals.

The GAC controller matrices $\mathbf{D}_1$ and $\mathbf{C}_1$ are calculated from

$$\mathbf{C}_1 = -\mathbf{R}_{f2}, \tag{16}$$

$$\mathbf{D}_1 = -\mathbf{R}_{f1}\underbrace{\left(\mathbf{J}^T(\mathbf{q}_{\text{cont}})\mathbf{K}_e\mathbf{J}(\mathbf{q}_{\text{cont}})\right)^{-1}}_{\tilde{\mathbf{K}}_e^{-1}}. \tag{17}$$

For 7-DOF manipulators, $\tilde{\mathbf{K}}_e$ is always singular and $\tilde{\mathbf{K}}_e\tilde{\mathbf{K}}_e^{+} \neq \mathbf{I}$ holds, because it is not possible to map a 6-dimensional Cartesian stiffness to a 7-dimensional joint-space. One independent information is always missing. Consequently $\mathbf{D}_1$ can be approximated by

$$\mathbf{D}_1 \approx -\mathbf{R}_{f1}\tilde{\mathbf{K}}_e^{+}. \tag{18}$$

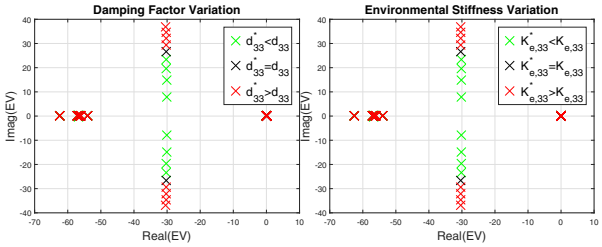

Fig. 2: Influence of CD eigenvalue configuration on damping parameter variation $d^*_{33} = k \cdot d_{33}$ (left column) and environmental stiffness parameter variation $K^*_{e,33} = k \cdot K_{e,33}$ (right column) with $k \in \mathbb{R}$ and $0.6 \leq k \leq 1.4$; Only imaginary part of weakly damped eigenvalue pair is affected by parameter variation

With the closed-loop dynamics (12) and its interpretation as a controlled fictive system (14), a dynamics analysis for predefined admittance controllers e.g. CD (see Subsection IV-B) and active controller synthesis (see Subsection IV-C) using linear control theory for the entire manipulator is possible.

B. Interpreting CD as special case of GAC

The CD structure (7) can be regarded as special case of GAC with

$$\boldsymbol{\xi} = \Delta\mathbf{q}_{\text{ref}},\ \mathbf{A}_1 = \mathbf{0},\ \mathbf{B}_1 = \mathbf{D}^{-1}\mathbf{S},\ \mathbf{C}_1 = \mathbf{I},\ \mathbf{D}_1 = \mathbf{0}. \tag{19}$$

Hence, the CD has a N_{dof}-dimensional integrator guaranteering steady-state convergence to constant reference forces and causing trajectory offset errors to the original planned TCP-trajectory after losing contact. Additionally this structure causes an eigenvalue pair with large imaginary part (see Figure 2). Hence, depending on the environmental stiffness and selected damping factor, significant oscillations can occur. This explains the well-known dilemma of tuning the damping matrix $\mathbf{D}$: the trade-off of reference response speed and acceptable oscillations.

C. GAC controller synthesis

For the active controller synthesis the *Complete Modal Control* (in German "Vollständige Modale Synthese") introduced in [18] is used (see also [19], [20], [21]). The Complete Modal Control is a parametric form of the eigenstructure assignment (see [22]). The controller matrix $\mathbf{R}_f$ is defined as

$$\mathbf{R}_f = -\mathbf{P}\mathbf{V}_R^{-1}, \tag{20}$$

where $\mathbf{V}_R$ is the (right-)eigenvector matrix $\mathbf{V}_R = [\mathbf{v}_{R1}, \ldots, \mathbf{v}_{Rn}]$ of the $\mathbf{R}_f$-controlled fictive system's eigenvalue problem

$$\left(\mathbf{A}_f - \mathbf{B}_f\mathbf{R}_f\right)\mathbf{v}_{Ri} = \lambda_{Ri}\mathbf{v}_{Ri}, \qquad i = 1, \ldots, n. \tag{21}$$

$\mathbf{P}$ is the parametervector matrix $\mathbf{P} = [\mathbf{p}_1, \ldots, \mathbf{p}_n]$ with additional degrees of freedom (DOF) in case of Multiple-Input-Multiple-Output systems. The relationship between eigen- and parametervectors is

$$(\lambda_{R_i}\mathbf{I} - \mathbf{A}_f)\mathbf{v}_{R_i} = \mathbf{B}_f\mathbf{p}_i. \tag{22}$$

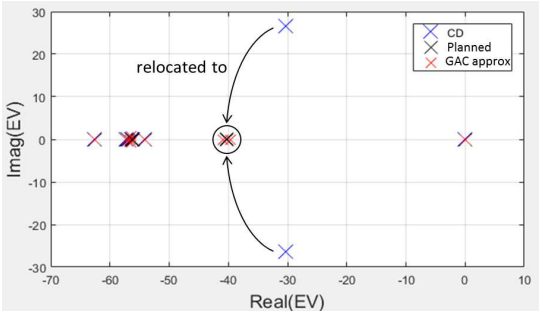

Fig. 3: Comparison of eigenvalue configuration: CD (blue), planned (black), GAC approx (red; taking (16), (18)); weakly damped CD eigenvalue pair is relocated to real axis by GAC; approximated solution of GAC causes a displacement of this damped eigenvalue pair

In summary, the controller's degrees of freedom are the closed-loop eigenvalues λ_{R_i} and the parametervectors $\mathbf{p}_i$ influencing the eigenvectors $\mathbf{v}_{R_i}$ corresponding to the eigenvalues λ_{R_i} in the subdimensional state-space[2] $\mathbf{G}_x(\lambda_{R_i}) = (\lambda_{R_i}\mathbf{I} - \mathbf{A}_f)^{-1}\mathbf{B}_f$. Hence, The parametervectors have an enormous influence on the entire closed-loop dynamics. They modify the internal system structure, e.g artificial dynamical coupling or decoupling of states can be achieved.

D. GAC parameter tuning

The question arises, how to define the degrees of freedom in form of eigenvalues and parametervectors properly to fulfill the closed-loop requirements of stability, performance and robustness. Indeed, a meaningful choice turns out to be challenging. Especially the choice of appropriate parametervectors is not self-explanatory. Additionally, in case of 7-DOF manipulators the closed-loop dynamics is not quadratic (number of outputs $\Delta\mathbf{q}_{ref}$ > number of inputs $\Delta\mathbf{f}$) which complicates the controller design.

The CD performance is good concerning stability, robustness and ease-of-use. Only the oscillations are disadvantageous. Therefore, it is meaningful to take over the CD closed-loop dynamics and damp the weakly damped eigenvalue pair to eliminate the oscillations (see Figure 3).

In case of 7-DOF manipulators, the approximation of $\mathbf{D}_1$ (18) causes a displacement of the planned eigenvalue configuration (black crosses in Figure 3). The internal structure of the closed-loop dynamics is kept by taking over the parametervectors of the CD structure.

Hence, it follows for the GAC matrices

$$\mathbf{A}_1 = \mathbf{0}, \quad \mathbf{B}_1 = \mathbf{D}^{-1}\mathbf{S}, \tag{23}$$

where $\mathbf{S}$ is the Cartesian selection matrix activating Cartesian compliance in desired Cartesian directions. For the definition of the eigenvalues and parametervectors following distinction of cases is done, where $\beta = 10^{-3}$ is used as threshold (compare Figure 3):

[2]This means that the parametervectors influence the partitioning of the eigendynamics $e^{(\lambda_{R_i}t)}$ to the states

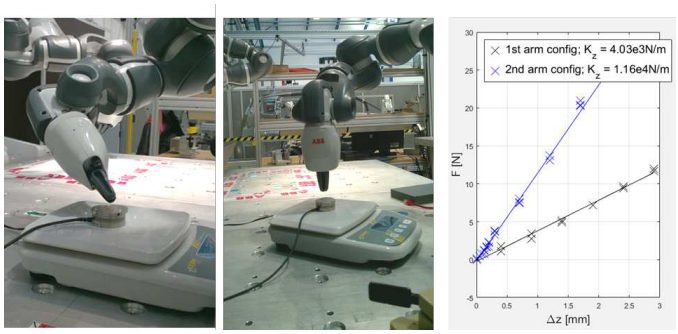

Fig. 4: Overview of ABB YuMi (7-DOF) joint configuration with different stiffness; Left: Moderate joint configuration; Middle: Stiff joint configuration; Right: Identified environmental stiffness $\mathbf{K}_e$ for both arm configurations

1) $\left|\text{imag}(\lambda_{Ri,\text{CD}})\right| < \beta$:

$$\lambda_{Ri,\text{GAC}} \overset{\text{def}}{=} \lambda_{Ri,\text{CD}}, \quad \mathbf{p}_{i,\text{GAC}} \overset{\text{def}}{=} \mathbf{p}_{i,\text{CD}}, \quad \mathbf{v}_{Ri,\text{GAC}} \overset{\text{def}}{=} \mathbf{v}_{Ri,\text{CD}}$$

2) $\text{imag}(\lambda_{Ri,\text{CD}}) \geq \beta$:

$$\lambda_{Ri,\text{GAC}} \overset{\text{def}}{=} -|\lambda_{Ri,\text{CD}}| \pm 10^{-3} i$$
$$\mathbf{p}_{i,\text{GAC}} \overset{\text{def}}{=} \mathbf{p}_{i,\text{CD}}, \; \mathbf{v}_{Ri,\text{GAC}} = (\lambda_{Ri,\text{GAC}}\mathbf{I} - \mathbf{A}_f)^{-1}\mathbf{B}_f\mathbf{p}_{i,\text{GAC}}$$

Considering the closed-loop system matrix $\mathbf{A}_g$ with (19), the CD eigenvalues and eigenvectors are calculated by

$$\mathbf{A}_{g,\text{CD}}\mathbf{v}_{Ri,\text{CD}} = \lambda_{Ri,\text{CD}}\mathbf{v}_{Ri,\text{CD}} \tag{24}$$

and the parametervectors by

$$(\lambda_{Ri,\text{CD}}\mathbf{I} - \mathbf{A}_f)\mathbf{v}_{Ri,\text{CD}} = \mathbf{B}_f\mathbf{p}_{i,\text{CD}}$$
$$\Downarrow$$
$$\begin{bmatrix} \lambda_{Ri,\text{CD}}\mathbf{I} - \mathbf{A}_{f,11} & \mathbf{0} \\ -\mathbf{A}_{f,21} & \lambda_{Ri,\text{CD}}\mathbf{I} \end{bmatrix} \begin{bmatrix} \mathbf{v}_{Ri,\text{CD},1} \\ \mathbf{v}_{Ri,\text{CD},2} \end{bmatrix} = \begin{bmatrix} \mathbf{B} \\ \mathbf{0} \end{bmatrix} \mathbf{p}_{i,\text{CD}}$$
$$\Downarrow$$
$$\mathbf{p}_{i,\text{CD}} = \mathbf{B}^{-1}(\lambda_{Ri,\text{CD}}\mathbf{I} - \mathbf{A}_{f,11})\mathbf{v}_{Ri,\text{CD},1}. \tag{25}$$

If all eigenvalues, eigen- and parametervectors are defined, the fictive state controller $\mathbf{R}_f$ can be calculated by (20) and consequently, the controller matrices $\mathbf{C}_1$ and $\mathbf{D}_1$ by (16) and (17), respectively.

V. Experimental Results

The proposed General Admittance Control (GAC) is implemented on the right arm of a 7-DOF ABB YuMi. The controller performance is compared to the classical Cartesian Damping structure (CD). For this, two joint configurations with different stiffness[1] $\mathbf{K}_e$ and different $\mathbf{q}_{\text{cont}}$ are choosen (see Figure 4). For each joint configuration the CD controller is tuned and the GAC parameters are calculated accordingly to Section IV-D. All relevant controller parameters are listed in Table I.

It is pointed out, that ABB YuMi is not equipped with a F/T sensor. Hence, a force observer introduced in [17] is implemented for contact force estimation. The observer includes a dead-zone filter avoiding controller reactions to noise effects. The 6-DOF force/torque sensor visible in Figure 4 (ATI mini40) is only used for validation purposes and not for closing the force control loop.

The experiment is organized as follows: A force ramp with $F_{z,\max} = -10N$ is selected as reference value. At $t = 4.5s$ the TCP starts rotating about the x-axis to check, if the controller is able to keep the reference force. Hence, this rotation can be interpreted as a disturbance.

In Figure 5 and Figure 6, the controllers' performances are compared to each other for the moderate joint and for the stiff joint configuration, respectively (see Figure 4). All controllers can achieve a stable TCP contact with the stiff environment even during the TCP rotation at $t > 4.5s$. But it is clearly observable that GAC has a better performance than CD. The first force undershoot is less and the force and TCP pose oscillations are reduced significantly. It seems if GAC has a dead-time and stationary force error. But both phenomenon are caused by the force observer and are discussed in the next paragraph. After this erroneously dead-time, the GAC speed is comparable to CD because of $|\lambda_{R,\text{GAC},1}| \approx |\lambda_{R,\text{CD},1}|$ and $|\lambda_{R,\text{GAC},2}| \approx |\lambda_{R,\text{CD},2}|$, respectively (see Table I). Hence, the theory fits to the experimental results.

For explanation of the erroneously dead-time and stationary inaccuracy in case of GAC the reference (black), estimated (blue) and measured (red) forces in z-direction are plotted in Figure 7. Additionally the force dead-zone area of the force observer (green) depending on the actual joint configuration (for more details we refer to [17]) is added to the reference force. Hence, if the estimated force is within this green marked area, than the force error as well as the controller output are equal zero. For GAC1 this is true for $0s < t < 1.1s$ and $1.7s < t < 4.5s$. The first time range results in the artifical dead-time between reference signal and plant reaction, the second one in a non-negligible stationary control error. Hence, both phenomenon are caused by the dead-zone filter and not by the controller itself. If a force sensor could be used for force feedback, both effects should be eliminated.

The drift error in x- and y-direction of GAC and CD are negligible and comparable to each other (see right columns in Figure 5 and Figure 6). For CD, the mapping from Cartesian to joint space is explicitly done online. In case of GAC this mapping is embedded, but the dependency of the Jacobian on the actual joint configuration $\mathbf{q}_{\text{act}}$ in (8)-(9) ensures, that the TCP moves only along the z-axis.

VI. Summary and Conclusion

In this paper, a new General Admittance Control (GAC) was introduced for force control of manipulators. With the GAC structure, the position controlled manipulator and the linearized contact force model it is possible to perform a systematical system analysis for existing admittance control structures like CD. Secondly, active controller synthesis can be done.

[1]The stiffness of the obstacle in z-direction is higher than the robot's stiffness and is therefore neglected.

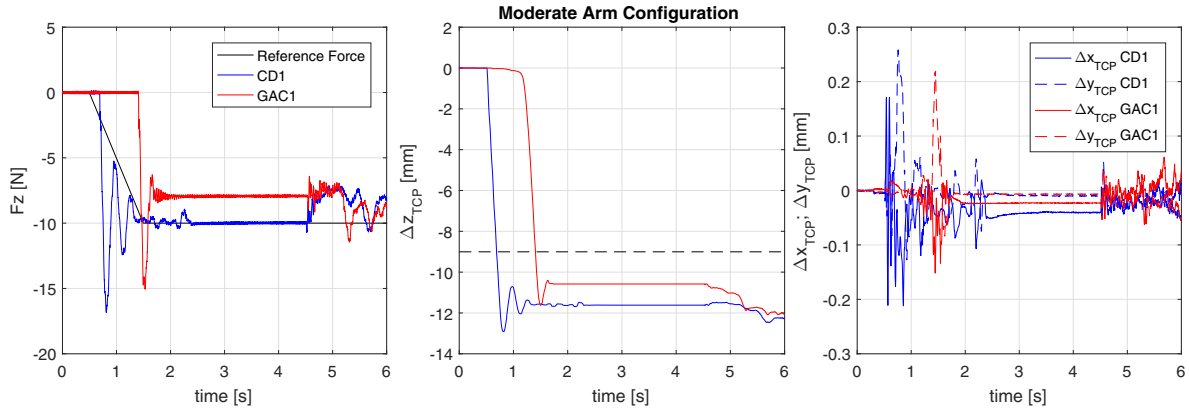

Fig. 5: Moderate arm configuration: Comparison of force controller performances of CD and GAC1 for free-traveling distance $H \approx -9mm$ (black dashed line); Left column: Measured force in z-direction; middle column: TCP displacement in z-direction; right column: TCP drift error in x- and y-direction

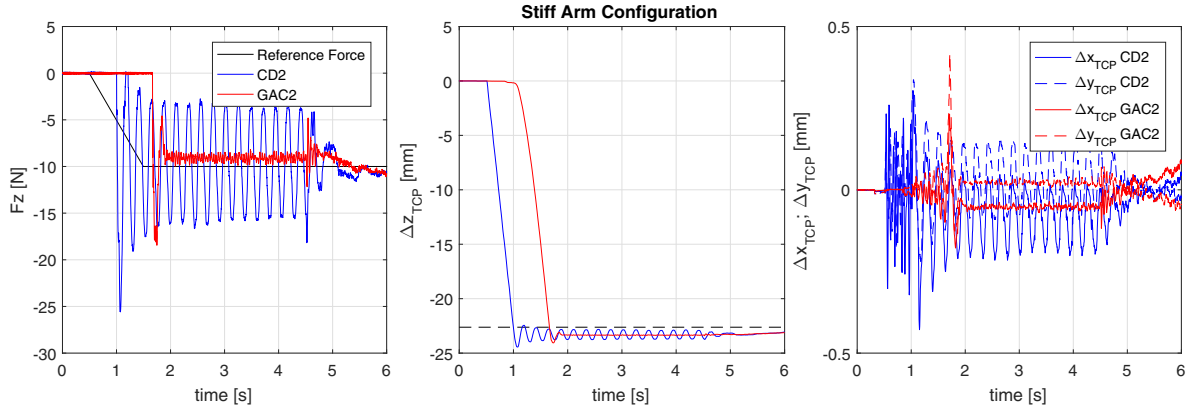

Fig. 6: Stiff arm configuration: Comparison of force controller performances of CD and GAC2 for free-traveling distance $H \approx -22.6mm$ (black dashed line); Left column: Measured force in z-direction; middle column: TCP displacement in z-direction; right column: TCP drift error in x- and y-direction

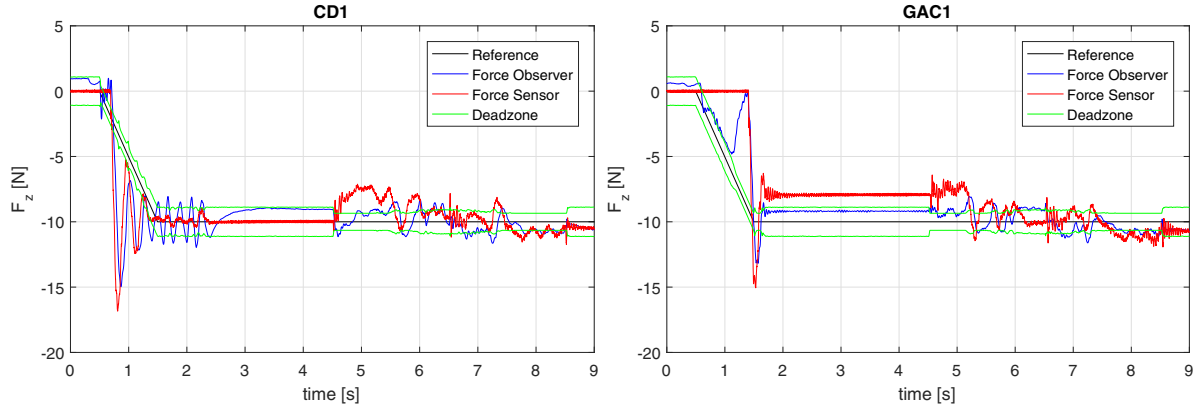

Fig. 7: Moderate arm configuration: Comparison of reference force (black), estimated force by Force Observer (blue) and measured force by 6-DOF force/torque sensor (red); force deadzone is adapted to actual joint configuration (green)

TABLE I: Summary of controller settings with corresponding eigenvalue configuration used for experiments in section V

Name	Controller Parameter Setting	Closed-loop Eigenvalues
Moderate Arm Configuration; $K_{e,33} = 4.03 \cdot 10^3$		
CD1	$d_{11} = d_{22} = 0.01$, $d_{33} = 0.0067$ $d_{44} = d_{55} = 0.4$, $d_{66} = 0.667$	$\lambda_{R,\mathrm{CD}} = -30.3 \pm 26.6i$, $\lvert\lambda_{R,\mathrm{CD}}\rvert = 40.3$
GAC1	$\lambda_{R,\mathrm{GAC}} = -40.3 \pm 10^{-3}i$	$\lambda_{R,\mathrm{GAC}} = \{-39.7, -40.9\}$
Stiff Arm Configuration; $K_{e,33} = 1.16 \cdot 10^4$		
CD2	$d_{11} = d_{22} = 0.01$, $d_{33} = 0.005$ $d_{44} = d_{55} = 0.4$, $d_{66} = 0.667$	$\lambda_{R,\mathrm{CD}} = -30.01 \pm 50.9i$, $\lvert\lambda_{R,\mathrm{CD}}\rvert = 59.1$
GAC2	$\lambda_{R,\mathrm{GAC}} = -59.1 \pm 10^{-3}i$	$\lambda_{R,\mathrm{GAC}} = -57.1 \pm 4.2i$

Here, the *Complete Modal Control* - a form of parametric eigenstructure assignment - was used. Consequently, the closed-loop eigenvalues and the internal state dynamics can be explicitly predefined. Hence, non-zero coupling effects in the position controlled manipulator can be taken into account. This is not possible with CD, as each Cartesian direction is considered independently in the controller design.

Using CD as a starting point, it was possible to take over all advantages of the CD structure while eliminating the disadvantageous oscillatory behavior. Therefore tuning the GAC can be done relative to the CD design and is therefore intuitive in the sense of ease-of-use. In the GAC approach, the mapping from Cartesian to joint-space is embedded. Although an explicit mapping as in CD is missing, the drift-error is negligible.

Contrary to CD the environmental stiffness and the joint configuration at first contact must be known for the GAC approach. In case of stiff contact situations the environmental stiffness can be approximated by the robot's stiffness which can be calculated by proper robot models if available. Otherwise the environmental stiffness must be identified beforehand which is disadvantageously in practice.

In case of 7-DOF manipulators, only an approximation of GAC can be calculated. Additionally, the contact forces are estimated by a force observer. Both disadvantages are expected to disappear if the GAC scheme is applied to a 6-DOF manipulator equipped with a F/T sensor.

REFERENCES

[1] R. Drath, B. Matthias, A. Horch, M. W. Krüger, and K. D. Listmann, "The internet of things, services and people," *atp edition*, vol. 58, pp. 36–43, 2016.

[2] C. Ott, R. Mukherjee, and Y. Nakamura, "A hybrid system framework for unified impedance and admittance control," *Journal of Intelligent and Robotic Systems*, vol. 78, no. 3, pp. 359–375, 2015.

[3] N. Hogan, "Impedance control: An approach to manipulation, part I – theory," *ASME Journal of Dynamic Systems, Measurement, and Control*, vol. 107, pp. 1–7, 1985.

[4] D. Lawrence, "Impedance control stability properties in common implementations," in *Proc. of IEEE International Conference on Robotics and Automation*, pp. 1185–1190, 1988.

[5] C. Ott, *Cartesian impedance control of redundant and flexible-joint robots*. Springer, 2008.

[6] B. Siciliano and O. Khatib, eds., *Springer Handbook of Robotics*. Springer, 2008.

[7] P. Labrecque and C. Gosselin, "Robotic force amplification with free space motion capability," in *Proc. of IEEE International Conference on Robotics and Automation*, pp. 134–140, 2014.

[8] A. Stolt, M. Linderoth, A. Robertsson, and R. Johansson, "Adaptation of force control parameters in robotic assembly," in *Proc. of IFAC International Symposium on Robot Control*, pp. 561–566, 2012.

[9] E. Villagrossi, *Robot dynamics modelling and control for machining applications*. PhD thesis, Universita degli Studi di Brescia, 2016.

[10] J. Roy and L. Whitcomb, "Adaptive force control of position/velocity controlled robots: Theory and experiments," *IEEE Transactions on Robotics and Automation*, vol. 18, no. 2, pp. 121–137, 2002.

[11] C.-H. Liang, S. Bhasin, K. Dupree, and W. Dixon, "A force limiting adaptive controller for a robotic system undergoing a noncontact-to-contact transition," *IEEE Transactions on Control Systems Technology*, vol. 17, no. 6, pp. 1330–1341, 2009.

[12] H. Wang, F. Patota, G. Buondonno, M. Haendl, A. De Luca, and K. Kosuge, "Stability and variable admittance control in the physical interaction with a mobile robot," *International Journal of Advanced Robotics*, vol. 12, no. 173, pp. 1–14, 2015.

[13] R. Kikuuwe, "A sliding-mode-like position controller for admittance control with bounded actuator force," *IEEE/ASME Transactions on Mechatronics*, vol. 19, no. 5, pp. 1489–1500, 2014.

[14] A. Wahrburg and K. D. Listmann, "Mpc-based admittance control for robotic manipulators," in *Proc. of IEEE Conference on Decision and Control*, pp. 7548–7554, 2016.

[15] J. Matschek, J. Bethge, P. Zometa, and R. Findeisen, "Force feedback and path following using predictive control: Concept and application to a lightweight robot," in *Proc. of IFAC World Congress*, pp. 10243–10248, 2017.

[16] A. Stolt, *On robotic assembly using contact force control and estimation*. PhD thesis, Lund University, 2015.

[17] A. Wahrburg, J. Bös, K. D. Listmann, F. Dai, B. Matthias, and H. Ding, "Motor-current-based estimation of cartesian contact forces and torques for robotic manipulators and its application to force control," *IEEE Transactions on Automation Science and Engineering*, 2017.

[18] G. Roppenecker, *Vollständige modale Synthese linearer Systeme und ihre Anwendung zum Entwurf strukturbeschränkter Zustandsrückführungen*. PhD thesis, Universität Karlsruhe, 1983.

[19] O. Föllinger, *Regelungstechnik - Einführung in die Methoden und ihre Anwendung*. Hüthig, 1994.

[20] U. Konigorski, "Pole placement by parametric output feedback," *Systems & Control Letters*, vol. 61, no. 2, pp. 292–297, 2012.

[21] E. Ostertag, *Mono- and Multivariable Control and Estimation*. Springer, 2011.

[22] M. Fahmy and J. O'Reilly, "Eigenstructure assignment in linear multivariable systems - a parametric solution," *IEEE Transactions on Automatic Control*, vol. 28, no. 10, pp. 990–994, 1983.